GEOPHYSICAL RESEARCH LETTERS, VOL. 33, L19605, doi:10.1029/2006GL027207, 2006

Global relationships of total alkalinity with salinity and temperature in surface waters of the world's oceans

Kitack Lee,[1] Lan T. Tong,[1] Frank J. Millero,[2] Christopher L. Sabine,[3] Andrew G. Dickson,[4] Catherine Goyet,[5] Geun-Ha Park,[1] Rik Wanninkhof,[6] Richard A. Feely,[3] and Robert M. Key[7]

Received 12 June 2006; revised 29 August 2006; accepted 5 September 2006; published 5 October 2006.

[1] A simple function of sea surface salinity (SSS) and temperature (SST) in the form $A_T = a + b\,(SSS - 35) + c\,(SSS - 35)^2 + d\,(SST - 20) + e\,(SST - 20)^2$ fits surface total alkalinity (A_T) data for each of five oceanographic regimes within an area-weighted uncertainty of ± 8.1 μmol kg^{-1} (1σ). Globally coherent surface A_T data (n = 5,692) used to derive regional correlations of A_T with SSS and SST were collected during the global carbon survey in the 1990s. Such region-specific A_T algorithms presented herein enable the estimation of the global distribution of surface A_T when observations of SSS and SST are available. **Citation:** Lee, K., L. T. Tong, F. J. Millero, C. L. Sabine, A. G. Dickson, C. Goyet, G.-H. Park, R. Wanninkhof, R. A. Feely, and R. M. Key (2006), Global relationships of total alkalinity with salinity and temperature in surface waters of the world's oceans, *Geophys. Res. Lett.*, *33*, L19605, doi:10.1029/2006GL027207.

1. Introduction

[2] Total alkalinity (A_T) variability in the surface ocean is controlled mainly by freshwater addition (precipitation and sea-ice melting) or removal (evaporation and sea-ice formation) which also acts to change salinity [*Brewer et al.*, 1986; *Millero et al.*, 1998a]. In the (Sub)tropical oceans (i.e., 30°N–30°S), surface A_T variations associated with water balance-induced changes in salinity account for more than ~80% of total variability in A_T [*Millero et al.*, 1998a]. At higher latitudes (i.e., north of ~30°N or south of ~30°S), a progressive increase in the convective mixing of deep waters rich in A_T during seasonal cooling is an important additional factor that acts to increase surface A_T concentrations. The greater the intensity of seasonal convective mixing; the higher the A_T associated with the dissolution of $CaCO_3$ and the lower the water temperature. In this case, A_T is negatively correlated with sea surface temperature. Coccolithophorid blooms during seasonal warming are key biological factors that decrease surface A_T in a measurable way [*Balch et al.*, 2005]. The formation and destruction of organic matter also impact surface A_T, but only in a minor way, except in biologically productive waters [*Kim et al.*, 2006]. Such decrease in A_T due to marine biota generally occurs in tandem with sea surface temperature increase. Overall, variations in both sea surface salinity (SSS) and temperature (SST) can be good proxies for surface A_T variations.

[3] Identifying the controls on surface A_T is becoming increasingly important for understanding the effects of ocean acidification resulting from the addition of anthropogenic CO_2 into surface waters [*Feely et al.*, 2004]. However, determining the global distribution of surface A_T is problematic because in many parts of the ocean A_T data are severely limited compared to the SSS and SST data sets, which are several orders of magnitude larger. In this case, empirical algorithms that relate surface A_T to SSS and SST are particularly useful in constructing the global distribution of A_T when combined with the global fields of SSS and SST. Such empirical A_T algorithms can aid in predicting the CO_2 flux across the air-sea interface in a numerical ocean model because surface pCO_2 could be calculated from the values of A_T and total inorganic carbon (C_T) for the model's surface box. In such a model, A_T and C_T are transported between the ocean boxes. Alternatively, surface pCO_2 and A_T data are used to calculate the surface C_T. The surface A_T algorithms can also be used to study other aspects of the marine carbonate system. For example, the annual cycle of A_T in the global ocean derived from the surface A_T algorithms along with hydrographic parameters can be extended to estimate the annual export production of biogenic $CaCO_3$ by integrating the seasonal decrease in the mixed-layer inventory of A_T, once it is corrected for salinity effects [*Lee*, 2001].

[4] The first set of global relationships of salinity-normalized A_T with SST [*Millero et al.*, 1998a] was derived using subsets (n = 1,740) of historical A_T data as well as those collected during the global carbon survey of the 1990s. Since the global A_T relationships first became available, a significant number of new A_T measurements have been added to the global data set. Here, we use surface A_T measurements (n = 5,692) from the Global Ocean Data Analysis Project v1.1 data set [*Key et al.*, 2004] which have been carefully quality controlled to determine the relationships of A_T with SSS and SST for different ocean regimes. The functional form of the model used in our analysis of surface A_T results is also distinct from that used by *Millero et al.* [1998a]. In the previous analysis, the equations that relate salinity-normalized A_T to SST probably include erroneous trends

[1] School of Environmental Science and Engineering, Pohang University of Science and Technology, Pohang, South Korea.
[2] Rosenstiel School of Marine and Atmospheric Science, University of Miami, Miami, Florida, USA.
[3] Pacific Marine Environmental Laboratory, NOAA, Seattle, Washington, USA.
[4] Scripps Institution of Oceanography, University of California, San Diego, La Jolla, California, USA.
[5] Biophysique et Dynamique des Systèmes Intégrés, Université de Perpignan, Perpignan, France.
[6] Atlantic Oceanographic Meteorological Laboratory, NOAA, Miami, Florida, USA.
[7] Program in Atmospheric and Oceanic Science, Princeton University, Princeton, New Jersey, USA.

0094-8276/06/2006GL027207$05.00

Table 1. Regional Representations of Surface Total Alkalinity (A_T) in the World's Oceans[a]

Zone	Ocean	Approximate Region[b]	A_T, μmol kg^{-1}	σ[c]	N[d]
1	(Sub)tropics[e]	30°S–30°N (Atlantic, Indian, and Pacific Oceans excluding Zone 2), SST > 20°C, 31 < SSS < 38	$2305 + 58.66\,(SSS - 35) + 2.32\,(SSS - 35)^2 - 1.41\,(SST - 20) + 0.040\,(SST - 20)^2$	8.6	2756
2	Equatorial upwelling Pacific	75°W–110°W → 20°N–20°S and 110°W–140°W → 10°N–10°S, SST > 18°C, 31 < SSS < 36.5	$2294 + 64.88\,(SSS - 35) + 0.39\,(SSS - 35)^2 - 4.52\,(SST - 29) - 0.232\,(SST - 29)^2$	7.5	644
3	North Atlantic	30°N–80°N, 0°C < SST < 20°C, 31 < SSS < 37	$2305 + 53.97\,(SSS - 35) + 2.74\,(SSS - 35)^2 - 1.16\,(SST - 20) - 0.040\,(SST - 20)^2$	6.4	326
4	North Pacific	north of 30°N, SST < 20°C, 31 < SSS < 35	$2305 + 53.23\,(SSS - 35) + 1.85\,(SSS - 35)^2 - 14.72\,(SST - 20) - 0.158\,(SST - 20)^2 + 0.062\,(SST - 20)\,(LONG)$	8.7	258
5	Southern Ocean	30°S–70°S, SST < 20°C, 33 < SSS < 36	$2305 + 52.48\,(SSS - 35) + 2.85\,(SSS - 35)^2 - 0.49\,(SST - 20) + 0.086\,(SST - 20)^2$	8.4	1708

[a]For predicting A_T from SSS and SST values in a given zone, the primary criterion for choosing an appropriate A_T algorithms is the SST. That is, when the temperature of a water sample in the zone of interest is out of the range of the applicable equation, the equation for an adjacent zone sharing a common boundary should be used instead.
[b]Geographic boundaries between the South Pacific–South Atlantic, between the South Atlantic–South Indian, and between the South Indian–South Pacific, are 70°W, 20°E, and 120°E, respectively.
[c]Root mean square deviation = $\{(\Delta)^2/(N - 1)\}^{0.5}$, where Δ is the difference between measured A_T values and those calculated from the equations.
[d]The number of data points used for fitting.
[e]Arabian Sea and Bay of Bengal are included.

[*Friis et al.*, 2003]. Therefore, for each ocean regime we relate A_T results to both SSS and SST.

2. Methods

2.1. Optimal Polynomial Model for Fitting A_T Data

[5] An optimal functional form for fitting A_T data for each ocean regime was chosen on the basis of results obtained from analysis of A_T data using the 10-fold cross validation method, which tests which polynomial form (first, second, or third order) gives a better fit [*Stone*, 1974; *Breiman*, 1996]. For each ocean regime, we randomly divided the A_T data set into 10 subsets. The first step of the 10-fold cross validation analysis was to remove 1 subset from the 10 data sets. Then we derived a regression model without this subset, predicted the output values for this subset using the derived regression model, and computed the residuals. This calculation routine was repeated for each subset and the squares of the resulting residuals were summed. This cross-validation analysis applied for polynomial models of first, second, and third order. We found that a second-order polynomial model yielded the lowest value of the sum of the squares of the residuals; hence we chose a second-order model as the optimal regression model for fitting A_T data for each ocean regime.

[6] We also tested whether the cross-correlation term between the two predictor variables (SSS and SST) should be included in the selected functional form. In all regimes, lower tolerance values (i.e., <0.2), calculated from $1 - r^2$ for the regression of the interaction term on SSS and SST, indicate a high correlation between the two predictor variables and their interactions. Therefore, the interaction term was not included in the polynomial model that was used for generating A_T algorithms. However, for the North Pacific, the model including the interaction term between SST and longitude significantly reduced systematic errors.

2.2. Global Surface A_T Data Used to Derive A_T Algorithms

[7] Global surveys of marine inorganic carbon parameter distributions were conducted from 1990 to 1998 as part of the Joint Global Ocean Flux Study, the Ocean Atmosphere Carbon Exchange Study, and the World Ocean Circulation Experiment. The final A_T data set is internally consistent to ±5 μmol kg^{-1} [*Key et al.*, 2004]. Detailed descriptions of measurement techniques and calibration procedures for A_T data are provided elsewhere [*Millero et al.*, 1998b; *Key et al.*, 2004]. Subsets (n = 5,692) of the final A_T data collected from waters of less than 20 m depth in the (Sub)tropics (i.e., 30°N–30°S) and 30 m depth at latitudes poleward of ~30° were used in deriving region-specific correlations of surface A_T with SSS and SST.

[8] Monthly mean global A_T fields on 1° latitude × 1° longitude grid cells were estimated from five regional A_T relationships presented in Table 1, along with monthly mean SSS and SST fields from the *World Ocean Atlas 2001* [*Conkright et al.*, 2002].

3. Results and Discussion

3.1. Parameterization of Alkalinity in Surface Oceans

[9] Our analysis indicates that the distribution of surface A_T can be derived by dividing the global ocean into five regimes with corresponding equations relating A_T to SSS and

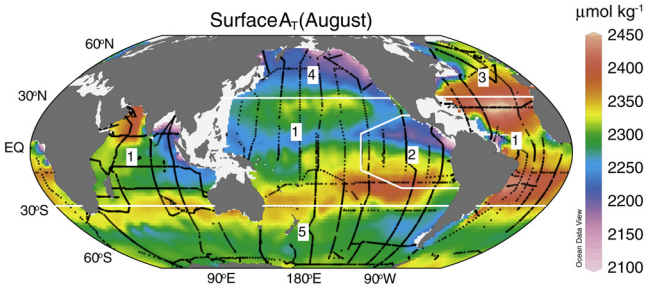

Figure 1. Monthly mean values of surface A_T (μmol kg^{-1}) for August for the world's ocean, as estimated from the regional A_T algorithms given in Table 1 applied to monthly mean sea surface salinity (SSS) and temperature (SST) fields (1° latitude × 1° longitude) from the *World Ocean Atlas 2001* [*Conkright et al.*, 2002]. White lines represent the approximate boundaries for the five different regions with unique relationships of A_T with SSS and SST and the numerical numbers represent the five regions listed in Table 1. Crosses denote locations of sampling stations.

SST (Table 1 and Figure 1). Since the derived equations given in Table 1 are expressed as functions of SSS and SST, the geographic boundaries of the regimes where the equations apply are dynamic, depending on seasonal variations in SST. For each ocean regime, surface A_T results are fitted to a second-order polynomial in SSS and SST and are also forced to satisfy equations for adjacent regime(s) which share boundaries with the regime of interest. The use of this functional form of equation is to ensure a smooth transition in A_T between adjacent regimes, and thus to minimize errors in A_T predictions at their mutual boundaries.

[10] In the (Sub)tropical oceans (Zone 1), except for the equatorial upwelling Pacific, waters with a temperature of 20°C and salinity of 35 have A_T values of about 2305 μmol kg^{-1} for the entire (Sub)tropics. Thus, at SST = 20°C and SSS = 35, A_T values in these warm waters are forced to an intercept of 2305 μmol kg^{-1} for the (Sub)tropics (see the first equation in Table 1). In the equatorial upwelling Pacific (Zone 2), waters have generally higher A_T values than those observed at the same salinity in similar latitude bands of the Atlantic and Indian Oceans. Thus, a separate equation is derived for this region to account for the effect of upwelling waters on the A_T trend. To make a smooth transition to values of A_T in the (Sub)tropics, the equation for this region is forced to an intercept of 2294 μmol kg^{-1} at SST = 29°C and SSS = 35. This intercept is similar to a mean A_T value for waters generally found at the boundary between the equatorial upwelling Pacific and the (Sub)tropics.

[11] In higher latitude oceans (poleward of 30°), regionally contrasting sets of coefficients are derived for equations of the same functional form for the North Atlantic (Zone 3), North Pacific (Zone 4), and Southern Ocean (Zone 5). In the North Pacific, the A_T values in the northwestern Pacific are significantly higher than those observed at the same salinity in the northeastern Pacific. Such contrasting trends of A_T in the North Pacific can be attributed to the east-west differences in the intensity of convective mixing. The greater the intensity of seasonal convective mixing; the higher the A_T. Therefore, the variable "longitude" is added to the equation to account for east-west A_T differences in the North Pacific (see the fourth equation in Table 1). The equations for the three zones at higher latitudes are all forced to the same intercept of 2305 μmol kg^{-1} at SST = 20°C and SSS = 35 to ensure a smooth transition to values of A_T in the (Sub)tropics.

[12] The effect of seasonal differences in A_T data on the derived A_T relationships was also addressed by comparing A_T values predicted from the relationships in Table 1 with A_T measurements which are not included in the data set. The mean difference of -1.2 ± 7.8 μmol kg^{-1} (1σ) indicates that the derived A_T relationships can be used to predict seasonal extrapolation of surface A_T. Some differences are found locally (Figure 2b), but these are still close to uncertainties of our A_T relationships (see the fifth column in Table 1). The effect of seasonality on the A_T relationships can be more thoroughly evaluated when time-series measurements become available in high latitude regions in which seasonal variations in both salinity and convective mixing lead to contrasting changes in surface A_T values, either in terms of magnitude or sign.

[13] For predicting A_T from SSS and SST values in a given zone, the primary criterion for choosing an appropriate A_T algorithm is the SST. That is, when the temperature of a water sample in the zone of interest is out of the range of the applicable equation, the equation for an adjacent zone sharing a common boundary should be used instead. For example, for

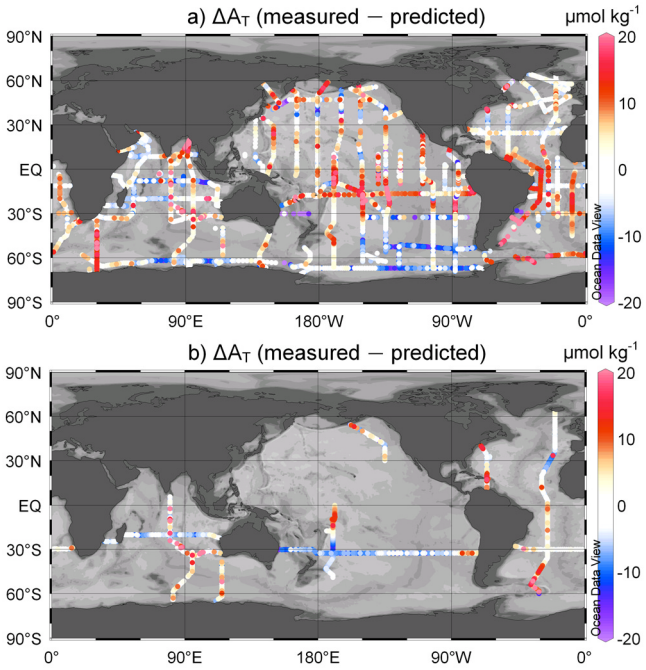

Figure 2. Comparison of the estimated A_T values from the regional A_T algorithms given in Table 1 with measurements which are (a) used or (b) not used when deriving the A_T algorithms. The measurements which are not used when deriving the A_T algorithms given Table 1 include data from the three major ocean basins: I8N/I8S (January 1995, along ~80°E), I03I04 (2003, along ~20°S), P06 (2003, along ~30°S), P15S/SR05 (2001, along ~170°E), P17N (2001, 135°W–160°W and 30°N–55°N), A10 (2003, along ~30°S), A16N/A16S (2003/2005, along ~20°W), and A22 (2003, along ~65°W).

waters with SST < 20°C, which are commonly found in the northern (Sub)tropical Atlantic (Zone 1) during the winter season, the equation that applies to the North Atlantic (Zone 3) should be used to predict A_T.

3.2. Global Distribution of Alkalinity in the Surface Ocean

[14] The global distribution of surface A_T for August calculated using the derived A_T algorithms of Table 1 applied to climatological SSS and SST fields [*Conkright et al.*, 2002] is shown in Figure 1. The surface A_T field shows broad maxima in the central gyres centered at about 25° north and south of the Equator, similar to the pattern for salinity. Such strong salinity-dependent trends in surface A_T result from the fact that the concentrations of the key chemical species (i.e., HCO_3^-, CO_3^{2-}, and $B(OH)_4^-$) that contribute to A_T proportionally increase with increasing salinity, and thus the ratio of A_T to salinity is approximately constant throughout the (Sub)tropics.

[15] Poleward of the (Sub)tropics, the annual excess precipitation over evaporation increases, and thus salinity decreases, with latitude. As a result, the values of A_T generally decrease with increasing latitude (Figure 1). Seasonal changes in the intensity of the convective mixing here are additional key factors that act to change surface A_T in a measurable way. During seasonal cooling, the intensive vertical mixing brings deep waters rich in $CaCO_3$-driven A_T to the surface, and thus increases surface A_T. During seasonal warming, however, the shoaling of the mixed layer makes the contribution of A_T-rich deep waters to the change in surface A_T minimal.

[16] The magnitude of seasonal A_T variability (Figure 3), computed by differencing the maximum and minimum monthly mean A_T values in each 1° latitude × 1° longitude grid cell, is directly proportional to the seasonal variations in salinity. Seasonal A_T variations are generally larger in the (Sub)tropics than in the higher-latitude oceans. In particular, larger amplitudes of seasonal variability are observed in areas where freshwater inputs through rivers (e.g., near the Amazon River and the Bay of Bengal) and the melting of ice (e.g., near sea-ice edges) are significant, or where tropical upwelling occurs.

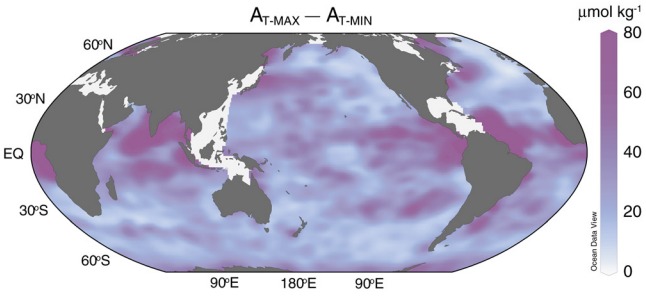

Figure 3. Distribution of the seasonal amplitude (maximum $A_{T\text{-}MAX}$ − minimum $A_{T\text{-}MIN}$) of surface A_T predicted from the regional A_T relationships given in Table 1, applied to monthly mean sea surface salinity and temperature fields (1° latitude × 1° longitude) from the *World Ocean Atlas 2001* [*Conkright et al.*, 2002].

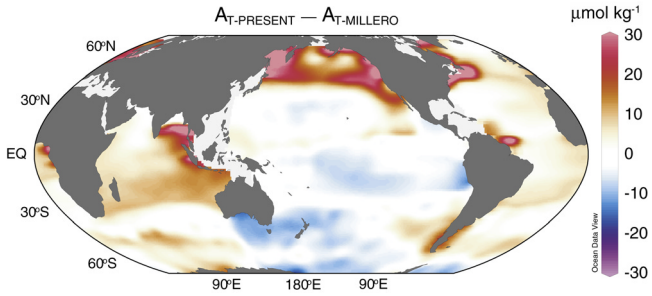

Figure 4. Differences (μmol kg^{-1}) in values of surface A_T for August determined from the regional A_T algorithms listed in Table 1, versus those calculated from previously reported A_T algorithms [*Millero et al.*, 1998a].

[17] Comparison of the surface A_T values for August calculated using the five equations (Table 1) applied to climatological SSS and SST fields with the corresponding values estimated using the algorithms previously reported by *Millero et al.* [1998a] reveals that the degree of discordance between the two sets of estimates varies regionally (Figure 4). The greatest differences are found in the North Pacific and the North Atlantic and, to a lesser extent, in the Southern Ocean. Non-negligible differences also are observed in the subtropical gyres of the South Pacific and South Indian Oceans. In the (Sub)tropics, *Millero et al.* [1998a] forced the single equation to two different intercepts for SST at 20°C; one for the northern and southern (Sub)tropical Pacific and another for the rest of (Sub)tropics. However, our analysis indicates that, regardless of basins, only a single intercept of the A_T equation is needed at SSS = 35 and SST = 20°C for the entire (Sub)tropics.

[18] Finally, since the five regional A_T algorithms given in Table 1 were derived from the most comprehensive surface A_T data available using the laboratory-calibrated measurement protocol, we propose that this new set of A_T equations should be used for the prediction of surface A_T over large oceanic areas where SSS and SST values are known.

[19] **Acknowledgments.** We thank all individuals who contributed to the global alkalinity data set, including the chief scientists. This work was financially supported by the National Research Laboratory Program of the Korea Science and Engineering Foundation. Partial support was provided by the AEBRC at the POSTECH, the Korea Aerospace Research Institute, the MOEHRD (KRF-2005-070-C00143), the Korea Science and Engineering Foundation (R01-2002-000-00549-0, 2004), and NOAA's Office of Climate Observation; PMEL contribution 2938.

References

Balch, W. M., H. R. Gordon, B. C. Bowler, D. T. Drapeau, and E. S. Booth (2005), Calcium carbonate measurements in the surface global ocean based on Moderate-Resolution Imaging Spectroradiometer data, *J. Geophys. Res.*, *110*, C07001, doi:10.1029/2004JC002560.

Breiman, L. (1996), Stacked regression, *Mach. Learn.*, *5*, 49–64.

Brewer, P. G., A. L. Bradshaw, and R. T. Williams (1986), Measurements of total carbon dioxide and alkalinity in the North Atlantic Ocean in 1981, in *The Changing Carbon Cycle: A Global Analysis*, edited by J. R. Trabalka and D. E. Reichle, pp. 348–370, Springer, New York.

Conkright, M. E., et al. (2002), *World Ocean Database 2001*, vol. 1, *Introduction*, edited by S. Levitus, *NOAA Atlas NESDIS 42*, 167 pp., NOAA, Silver Spring, Md.

Feely, R. A., C. L. Sabine, K. Lee, W. Berelson, J. Kleypas, V. J. Fabry, and F. J. Millero (2004), Impact of anthropogenic CO_2 on the $CaCO_3$ system in the oceans, *Science*, *305*, 362–366.

Friis, K., A. Kortzinger, and D. W. R. Wallace (2003), The salinity normalization of marine inorganic carbon chemistry data, *Geophys. Res. Lett.*, *30*(2), 1085, doi:10.1029/2002GL015898.

Key, R. M., et al. (2004), A global ocean carbon climatology: Results from Global Data Analysis Project (GLODAP), *Global Biogeochem. Cycles*, *18*, GB4031, doi:10.1029/2004GB002247.

Kim, H.-C., K. Lee, and W. Choi (2006), Contribution of phytoplankton and bacterial cells to the measured alkalinity of seawater, *Limnol. Oceanogr.*, *51*, 331–338.

Lee, K. (2001), Global net community production estimated from the annual cycle of surface water total dissolved inorganic carbon, *Limnol. Oceanogr.*, *46*, 1287–1297.

Millero, F. J., K. Lee, and M. Roche (1998a), Distribution of alkalinity in the surface waters of the major oceans, *Mar. Chem.*, *60*, 111–130.

Millero, F. J., et al. (1998b), Assessment of the quality of the shipboard measurements of total alkalinity on the WOCE hydrographic program Indian Ocean CO_2 survey cruises 1994–1996, *Mar. Chem.*, *63*, 9–20.

Stone, M. (1974), Cross validatory choice and assessment of statistical predictions, *J. R. Stat. Soc., Ser B.*, *36*, 117–147.

A. G. Dickson, Scripps Institution of Oceanography, University of California, San Diego, 9500 Gilman Drive, La Jolla, CA 92093-0244, USA.

R. A. Feely and C. L. Sabine, Pacific Marine Environmental Laboratory, NOAA, Seattle, WA 98115-0070, USA.

C. Goyet, Biophysique et Dynamique des Systèmes Intégrés, Université de Perpignan, 52 avenue Paul Alduy, F-66860 Perpignan, France.

R. M. Key, Program in Atmospheric and Oceanic Science, Princeton University, Forrestal Campus/Sayre Hall, Princeton, NJ 08544, USA.

K. Lee, G.-H. Park, and L. T. Tong, School of Environmental Science and Engineering, Pohang University of Science and Technology, San 31, Hyoja-dong, Nam-gu, Pohang 790-784, South Korea. (ktl@postech.ac.kr)

F. J. Millero, Rosenstiel School of Marine and Atmospheric Science, University of Miami, Miami, FL 33149, USA.

R. Wanninkhof, Atlantic Oceanographic Meteorological Laboratory, NOAA, 4301 Rickenbacker Causeway, Miami, FL 33149, USA.